Research Article ISSN: 2836-3647

American Journal of Pathology & Research

Ab Initio Whole Cell Kinetic Model of Bifidobacterium longum subsp. longum JCM1217 (blmSHM26)

Shnan Harish Modankap[1,2], Shamsia Bte Ali[1,2], Jullean Louise Dizon Baylon[1,2], Lavanya Dhingra[1,2], Nurhaliza Mohamed Ali[1,2], Parkavi Subramanian[1,2] and Maurice Han Tong Ling[2,3,4*]

[1]*Department of Applied Sciences, Northumbria University, United Kingdom.*

[2]*Management Development Institute of Singapore, Singapore.*

[3]*Newcastle Australia Institute of Higher Education, University of Newcastle, Australia.*

[4]*HOHY PTE LTD, Singapore.*

***Correspondence:**
Maurice Han Tong Ling, Management Development Institute of Singapore, Singapore, Newcastle Australia Institute of Higher Education, University of Newcastle, Australia.

Received: 14 Jul 2026; **Accepted:** 17 Aug 2026; **Published:** 31 Aug 2026

Citation: Shnan Harish Modankap, Shamsia Bte Ali, Jullean Louise Dizon Baylon, et al. Ab Initio Whole Cell Kinetic Model of Bifidobacterium longum subsp. longum JCM1217 (blmSHM26). American J Pathol Res. 2026; 5(8): 1-5.

ABSTRACT

Bifidobacterium longum subsp. longum JCM 1217 (= ATCC 15707; = DSM32940) is an important probiotic that is involved in human milk oligosaccharide metabolism, gut homeostasis and immune regulation. Despite its biological significance, no whole cell kinetic model has previously been developed for this strain. This study developed the first ab initio kinetic model for B. longum JCM 1217 using annotated genome and biochemical reaction information was obtained from National Center for Biotechnology Information (NCBI) and Kyoto Encyclopedia of Genes and Genomes (KEGG) respectively. The metabolic network was reconstructed using the AdvanceSyn Toolkit, wherein the model represented a system of ordinary differential equations (ODEs) which incorporated Michaelis-Menten kinetics together with transcription and translation rate laws. The final model consists of 753 enzymatic reactions, 327 enzymes and 731 metabolites and was successfully simulated, showing model validity and potential prediction of dynamic intracellular metabolism.

Keywords

Kinetic modelling, Metabolic network reconstruction, Michaelis–Menten kinetics, Ordinary differential equations, Human milk oligosaccharides, Gut homeostasis, Systems biology.

Introduction

The genus *Bifidobacterium* comprises Gram-positive anaerobes with a bifurcated Y-shaped cellular morphology and are the earliest colonisers of the human gastrointestinal tract. Taxonomically classified within the phylum Actinomycetota, bifidobacteria are characterised with a high genomic G+C content (~60-67 mol%) and employ a bifid shunt yielding acetate and lactate as metabolic products. It confers a metabolic efficiency that surpasses the classic lactic acid bacteria [1]. Originally isolated from the human intestine, *Bifidobacterium longum* subsp. *longum* JCM 1217 (BLM) is a fully genome-sequenced type strain that is widely distributed across the human lifespan, colonising the neonatal gut and persisting in diminished proportions into adulthood [2]. Markedly, BLM utilises human milk oligosaccharides (HMOs), complex glycans derived from breast milk [3,4]. Protein engineering of lacto-N-biosidase, encoded by this strain, has enabled production of complex HMO derivatives; expanding HMO-derived infant formula portfolio and promising for glycan-based therapeutics [5].

Furthermore, the capacity of extracellular alpha-L-arabinofuranosidase to degrade arabinoxylan and arabinan from cereal-derived plant cell wall expands the range of prebiotic substrates and reinforces its probiotic potential [6]. BLM also encodes a glucanotransferase whose action on potato starch produces a thermoreversible gel, relevant in food texture engineering [7]. BLM's therapeutic relevance extends further via the production of endo-α-N-acetylgalactosaminidase (EngBF), which cleaves tumour-associated antigen from the surface of mucin-type

glycoproteins overexpressed in epithelial cancers, aiding in CAR-T cell therapy [8,9]. The same enzyme EngBF additionally catalyses transglycosylation of disaccharides into bioactive peptides, emphasising its role as a precision biocatalyst for glycopeptide synthesis [9]. Aside from its enzymatic significance, Fukuda et al. demonstrated that acetate production by BLM, upregulated host immunomodulatory genes leading to complete protection against enteropathogens [10]. Due to *B. longum*'s lack of endotoxin, its ability of mucosal adhesion, and high bio-compatibility, emerging research could highlight its potential as an oral vaccine and *in situ* secretion of therapeutic enzymes [11].

Despite the substantial biochemical and genome sequencing knowledge and genome-scale metabolic reconstructions for BLM, no kinetic mathematical model has been reported to date. Genome-Scale Models (GSM) of type strains have clarified HMO utilisation pathways under steady state assumptions but are inherently unable to capture dynamic metabolic transitions [12,13]. However, Kinetic Models (KM) enable identification of rate limiting steps and control points that are generally not identified from stoichiometric models alone [14], resulting in predictive engineering that can evaluate gene knockouts or overexpression outcomes and test regulatory hypotheses in silico before experimental validation [15]. Hence, this study aims to construct a KM of *B. longum* JCM 1217 using *ab initio* approach by identifying enzymes from its annotated genome, and identifying the corresponding reaction from KEGG [16]. The result is a whole cell KM of *B. longum* JCM 1217, named as blmSHM26 using the nomenclature proposed by Cho and Ling [17], which consists of 731 metabolites, 327 enzymes with corresponding transcriptions and translations, and 753 enzymatic reactions.

Materials and Methods

Identification of Reactome

The reference genome of *Bifidobacterium longum* subsp. *longum* JCM 1217 was obtained from the NCBI GenBank database where it is archived under the assembly accession GCF_000196555.1 (accession numbers AP010888 and NC_015067) [10]. The genome assembly was used as the primary reference to identify enzymatic genes focusing on complete Enzyme Commission (EC) number was mapped to its corresponding reaction identifier using the KEGG LIGAND database for enzyme nomenclature. For example, EC 1.1.1.23 catalyses reactions 401158, R01163, and R03012, wherein substrates and products of each reaction can be identified.

Model Development

The model was developed using the ODE formats described in Sim et al. [18]. To represent transcription and translation within the kinetic model, *Escherichia coli* was used as a reference organism, as its gene expression parameters have been extensively characterised and are available in the Bionumbers database. For transcription, *E. coli* contains approximately 3,000 RNA polymerase molecules per cell (BioNumbers 106199), of which ~25% are transcriptionally active (BioNumbers 11676) [19], elongating at a rate of 22 nucleotides per second (BioNumbers 104109) [20]. Given an average ribonucleotide mass of 339.5 Da and the total mRNA synthesis per *E. coli* cell is estimated as 5,600 kDA per second, this corresponds to 9.3e-18 grams per second. Normalised to an *E. coli* cell volume of about 0.7 cubic micrometres [21] and 4,225 coding genes (BioNumbers 105443) [22], this yields an average transcription rate of 2.92 μM per protein-coding gene per second or 2.92e-03 mM. With an average mRNA lifetime of 1.79 minutes (107.56 seconds) (BioNumbers 107666) [23], corresponding to a degradation rate constant of 0.0093 per second (0.93% decay per second). Consequently, mRNA concentration was modelled as a first-order process: d[mRNA]/dt = 0.00292 - 0.0093[mRNA]. Protein translation was modelled using a median rate of 1,000 peptides per mRNA transcript per hour (BioNumbers 106382) [24], equivalent to 0.278 peptides per mRNA transcript per second [25]. Protein degradation in *E. coli* was assumed to occur at approximately 1% per hour (BioNumbers 109924) [26], corresponding to a degradation constant of 2.78e-06 per second. Protein concentration was accordingly described by: d[Protein]/dt = 0.278[mRNA] - 2.78e-06[Protein]. The reactome as such was represented using ODEs [27] with enzyme parameters from Bar-Even et al.'s median survey [28] and formatted to meet AdvanceSyn Model Specification criteria [29].

Model Simulation

The constructed model was tested for simulatability using AdvanceSyn Toolkit [29]. Initial concentrations of all mRNA species and enzymes were set to 0 mM. Most metabolites concentrations were initialised at 1 mM. However, a subset of metabolites were assigned an initial concentration of 1000 mM to ensure their availability through the simulation: (i) water (C00001), (ii) ATP (C00002), (iii) NAD^+ (C00003), (iv) NADH (C00004), (v) NADPH (C00005), (vi) $NADP^+$ (C00006), (vii) ADP (C00008), (viii) Carbon dioxide (C00011), (ix) L-Glutamate (C00025), (x) D-Glucose (C00031 and C00092), (xi) Glycine (C00037), (xii) L-Alanine (C00041), (xiii) L-Lysine (C00047), (xiv) L-Aspartate (C00049), (xv) L-Arginine (C00062), (xvi) L-Glutamine (C00064), (xvii) L-Serine (C00065), (xviii) L-Methionine (C00073), (xix) L-Tryptophan (C00078), (xx) L-Phenylalanine (C00079), (xxi) L-Tyrosine (C00082), (xxii) L-Cysteine (C00097), (xxiii) L-Leucine (C00123), (xxiv) D-Alanine (C00133), (xxv) L-Histidine (C00135), (xxvi) L-Proline (C00148), (xxvii) L-Valine (C00183), (xxviii) L-Threonine (C00188), (xxix) D-Glutamate (C00217), (xxx) L-Isoleucine (C00407), (xxxi) D-Serine (C00740), and (xxxii) D-Glutamine (C00819). Model simulation was performed from time 0 to 3600 seconds time period to examine temporal changes in metabolite concentrations using fourth-order Runge-Kutta method [30,31]. A simulation timestep of 0.1 seconds was employed, and metabolite concentrations were constrained to the 0 millimolar to 1000 millimolar range throughout the simulate on. Simulation outputs were sampled at 2 second intervals.

Results and Discussion

Using the annotated genome of BLM, a kinetic model was developed from 2009 genes, where 1924 are protein-coding

genes. 1,050 EC numbers, which contained uniquely identifiable reactions, were associated with 753 enzymatic reactions, involving 327 enzymes and 731 metabolites allowing development on the basis of specifications for AdvanceSyn Toolkit models [29]. Additionally, 654 ODEs acting as a placeholder for enzyme transcription and translation were added.

The successful execution of the model, as simulated via the AdvanceSyn Toolkit [29] (Figure 1), is validated against two criteria: the absence of syntax or compilation errors, which confirms the correct model construction, and the generation of simulation results, which confirms the model's simulatability. The validation is further substantiated by the visual representation of fluctuations instead of flatlining within the graphs of simulated metabolite concentrations denoting a significant response to the presence of other metabolites (a network) rather than independent behaviour. As the simulation output is governed by median rather than enzyme-specific kinetic constants [31], these results are interpreted in line with the framing adopted in recent comparable models [32-36]. These form the foundation on which biologically representative parameters can be built. On this basis, the central achievement of this study is the establishment of a fully functioning whole-cell kinetic model for *B. longum* JCM 1217, a flexible template for future expansion by incorporating growth coupling, variable enzyme kinetics, and even as a system to explore resource allocation within the cellular environment [37-41].

Conclusion

The study presents the first *ab initio* whole cell kinetic model of *Bifidobacterium longum* subsp. *longum* JCM 1217 (blmSHM26), comprising 731 metabolites, 327 enzymes with transcriptions and translations, and 753 enzymatic reactions.

Supplementary Materials

Reaction descriptions and model can be download from https://bit.ly/blmSHM26.

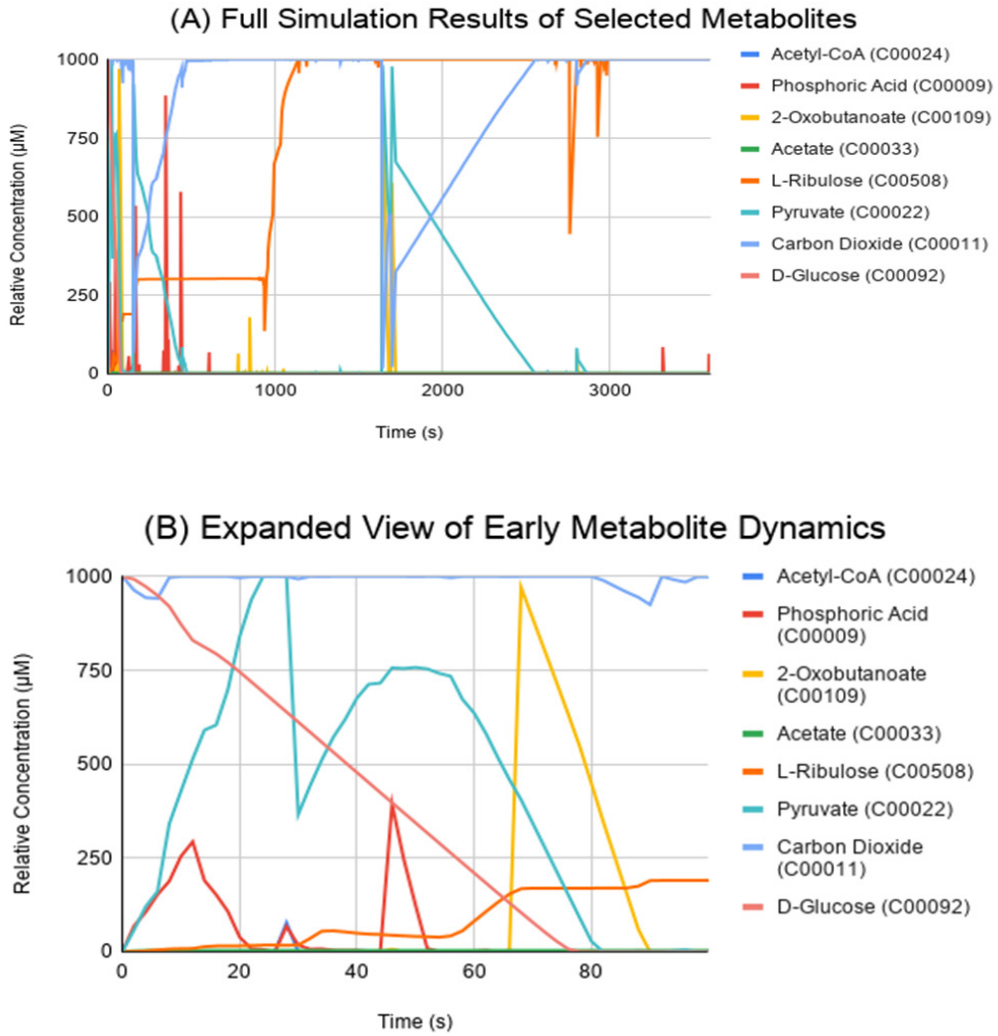

Figure 1: Full simulation results of selected metabolites against time. Panel A shows full simulation results (3600 seconds) while Panel B zooms into 0 to 100 seconds.

Acknowledgements

The authors wish to thank the institute, Management Development Institute of Singapore, for its support towards this work. The cost of publication fees was borne by the authors.

References

1. O'Callaghan A, Van Sinderen D. Bifidobacteria and Their Role as Members of the Human Gut Microbiota. Front Microbiol. 2016; 7: 925.
2. Odamaki T, Bottacini F, Kato K, et al. Genomic diversity and distribution of Bifidobacterium longum subsp. longum across the human lifespan. Sci Rep. 2018; 8: 85.
3. Turroni F, Peano C, Pass DA, et al. Diversity of Bifidobacteria within the Infant Gut Microbiota. PLoS One. 2012; 7: e36957.
4. Shao Y, Wang S, Gichuki BM, et al. Genomic atlas of Bifidobacterium infantis and B. longum informs infant probiotic design. Cell. 2026; 189: 1854-1873.e17.
5. Vuillemin M, Lengyel M, Muschiol J, et al. Enzymatic lacto-N-biose elongation of human milk oligosaccharides with the GH136 lacto-N-biosidase LnbX engineered for improved transglycosylation. Enzyme Microb Technol. 2025; 189: 110660.
6. Friess L, Bottacini F, McAuliffe FM, et al. Two extracellular α-arabinofuranosidases are required for cereal-derived arabinoxylan metabolism by Bifidobacterium longum subsp. longum. Gut Microbes. 2024; 16: 2353229.
7. Jeong D-W, Jeong H-M, Shin Y-J, et al. Properties of recombinant 4-α-glucanotransferase from Bifidobacterium longum subsp. longum JCM 1217 and its application. Food Sci Biotechnol. 2020; 29: 667-674.
8. Ashida H, Ozawa H, Fujita K, et al. Syntheses of mucin-type O-glycopeptides and oligosaccharides using transglycosylation and reverse-hydrolysis activities of Bifidobacterium endo-α-N-acetylgalactosaminidase. Glycoconj J. 2010; 27: 125-132.
9. Suzuki R, Katayama T, Kitaoka M, et al. Crystallographic and Mutational Analyses of Substrate Recognition of Endo-α-N-acetylgalactosaminidase from Bifidobacterium longum. J Biochem. 2009; 146: 389-398.
10. Fukuda S, Toh H, Hase K, et al. Bifidobacteria can protect from enteropathogenic infection through production of acetate. Nature. 2011; 469: 543-547.
11. Kitagawa K, Oda T, Saito H, et al. Development of oral cancer vaccine using recombinant Bifidobacterium displaying Wilms' tumor 1 protein. Cancer Immunol Immunother. 2017; 66: 787-798.
12. Román L, Melis-Arcos F, Pröschle T, et al. Genome-scale metabolic modeling of the human milk oligosaccharide utilization by Bifidobacterium longum subsp. infantis. mSystems. 2024; 9: e00715-23.
13. Lee YQ, Choi Y-M, Park S-Y, et al. Genome-scale metabolic model-guided systematic framework for designing customized live biotherapeutic products. NPJ Syst Biol Appl. 2025; 11: 73.
14. Srinivasan S, Cluett WR, Mahadevan R. Constructing kinetic models of metabolism at genome-scales: A review. Biotechnol J. 2015; 10: 1345-1359.
15. Toumpe I, Choudhury S, Hatzimanikatis V, et al. The Dawn of High-Throughput and Genome-Scale Kinetic Modeling: Recent Advances and Future Directions. ACS Synth Biol. 2025; 14: 2906-2919.
16. Okuda S, Yamada T, Hamajima M, et al. KEGG Atlas mapping for global analysis of metabolic pathways. Nucleic Acids Res. 2008; 36: W423-W426.
17. Cho JL, Ling MHT. Adaptation of Whole Cell Kinetic Model Template, UniKin1, to Escherichia coli Whole Cell Kinetic Model, ecoJC20. EC Microbiology. 2021; 17.2: 254-260.
18. Sim BJH, Tan NTF, Ling MHT. Multilevel Metabolic Modelling Using Ordinary Differential Equations. Encyclopedia of Bioinformatics and Computational Biology (Elsevier). 2025; 491-498.
19. Klumpp S, Hwa T. Growth-rate-dependent partitioning of RNA polymerases in bacteria. Proc Natl Acad Sci U S A. 2008; 105: 20245-20250.
20. Gray WJH, Midgley JEM. The control of ribonucleic acid synthesis in bacteria. The synthesis and stability of ribonucleic acid in rifampicin-inhibited cultures of Escherichia coli. Biochem J. 1971; 122: 161-169.
21. Kubitschek HE, Friske JA. Determination of bacterial cell volume with the Coulter Counter. J Bacteriol. 1986; 168: 1466-1467.
22. Blattner FR, Plunkett G, Bloch CA, et al. The Complete Genome Sequence of Escherichia coli K-12. Science. 1997; 277: 1453-1462.
23. So L, Ghosh A, Zong C, et al. General properties of transcriptional time series in Escherichia coli. Nat Genet. 2011; 43: 554-560.
24. Schwanhäusser B, Busse D, Li N, et al. Corrigendum: Global quantification of mammalian gene expression control. Nature. 2013; 495: 126-127.
25. Maurizi MR. Proteases and protein degradation inEscherichia coli. Experientia. 1992; 48: 178-201.
26. Larrabee KL, Phillips JO, Williams GJ, et al. The relative rates of protein synthesis and degradation in a growing culture of Escherichia coli. J Biol Chem. 1980; 255: 4125-4130.
27. Murthy MV, Balan D, Kamarudin NJ, et al. UniKin1: A Universal, Non-Species-Specific Whole Cell Kinetic Model. Acta Scientific Microbiology. 2020; 3.10: 04-08.
28. Bar-Even A, Noor E, Savir Y, et al. The Moderately Efficient Enzyme: Evolutionary and Physicochemical Trends Shaping Enzyme Parameters. Biochemistry. 2011; 50: 4402-4410.
29. Ling MHT. AdvanceSyn Toolkit:An open-source suite for model development and analysis in biological engineering. MOJ Proteomics Bioinform. 2020; 9: 83-86.

30. Butcher JC. Numerical Methods for Ordinary Differential Equations (Wiley), 1st Ed. 2008.
31. Yong B. The Comparison of Fourth Order Runge-Kutta and Homotopy Analysis Method for Solving Three Basic Epidemic Models. Journal of Physics Conf Series. 2019; 1317: 012020.
32. Ling MHT. Ab Initio Whole Cell Kinetic Model of Streptococcus equi subsp. zooepidemicus SEZ13 (seqSA26). Scholastic Medical Sciences. 2026; 3.6: 02-04.
33. Ling MHT, Yeo KY, Arivazhagan M, et al. Ab Initio Whole Cell Kinetic Model of Yarrowia lipolytica CLIB122 (yliYKY24). Medicon Medical Sciences. 2025; 8: 13-18.
34. Ling MHT, Wong TB, Le MA, et al. Ab Initio Whole Cell Kinetic Models of Escherichia coli BL21 (ebeTBSW25) and MG1655 (ecoMAL25). Scholastic Medical Sciences. 2025; 2.2: 01-04.
35. Ling MHT, Senthilkumar A, Arivazhagan M, et al. Ab Initio Whole Cell Kinetic Model of Lactobacillus acidophilus NCFM (lacAS24). J Clin Immunol Microbiol. 2025; 6: 1-5.
36. Ling MHT, Arivazhagan M, Senthilkumar A, et al. Ab Initio Whole Cell Kinetic Model of Bifidobacterium bifidum BGN4 (bbfMA24). Acta Scientific Nutritional Health. 2025; 9.1: 42-45.
37. Stalidzans E, Seiman A, Peebo K, et al. Model-based metabolism design: constraints for kinetic and stoichiometric models. Biochem Soc Trans. 2018; 46: 261-267.
38. Ahn-Horst TA, Mille LS, Sun G, et al. An expanded whole-cell model of E. coli links cellular physiology with mechanisms of growth rate control. NPJ Syst Biol Appl. 2022; 8: 30.
39. Hao T, Song Z, Zhang M, et al. Reconstruction of Metabolic–Protein Interaction Integrated Network of Eriocheir sinensis and Analysis of Ecdysone Synthesis. Genes. 2024; 15: 410.
40. Bianchi DM, Pelletier JF, Hutchison CA, et al. Toward the Complete Functional Characterization of a Minimal Bacterial Proteome. J Phys Chem B. 2022; 126: 6820-6834.
41. Baldazzi V, Ropers D, Gouzé J-L, et al. Resource allocation accounts for the large variability of rate-yield phenotypes across bacterial strains. eLife. 2023; 12: e79815.